*Immunology* 2003 **108** 70–78

# Mycobacteria, an environmental enhancer of lupus nephritis in a mouse model of systemic lupus erythematosus

CHRISTINE G. HAWKE,* DOROTHY M. PAINTER,† PAUL D. KIRWAN,‡ ROSEMARY R. VAN DRIEL,§ & ALAN G. BAXTER* **Autoimmunity Research Group, Centenary Institute of Cancer Medicine and Cell Biology, Newtown NSW, Australia., †(Deceased) Department of Anatomical Pathology, Royal Prince Alfred Hospital, Camperdown NSW, Australia, ‡Central Sydney Area Health Service, Electron Microscopy Department, Concord Repatriation and General Hospital, Concord NSW, Australia and §IATIA Ltd., Box Hill, Victoria, Australia*

## SUMMARY

Systemic lupus erythematosus (SLE) is a chronic systemic autoimmune disease characterized by the production of antibodies directed against self antigens. Immune complex glomerulonephritis (GN) is one of the most serious complications of this disorder and can lead to potentially fatal renal failure. The aetiology of SLE is complex and multifactorial, characterized by interacting environmental and genetic factors. Here we examine the nature of the renal pathology in mycobacteria-treated non-obese diabetic (NOD) mice, in order to assess its suitability as a model for studying the aetiopathogenesis of, and possible treatment options for, lupus nephritis (LN) in humans. Both global and segmental proliferative lesions, characterized by increased mesangial matrix and cellularity, were demonstrated on light microscopy, and lesions varied in severity from very mild mesangiopathic GN through to obliteration of capillary lumina and glomerular sclerosis. Mixed isotype immune complexes (IC) consisting of immunoglobulin G (IgG), IgM, IgA and complement C3c were detected using direct immunofluorescence. They were deposited in multiple sites within the glomeruli, as confirmed by electron microscopy. The GN seen in mycobacteria-treated NOD mice therefore strongly resembles the pathology seen in human LN, including mesangiopathic, mesangiocapillary and membranous subclasses of LN. The development of spontaneous mixed isotype IC in the glomeruli of some senescent NOD mice suggests that mycobacterial exposure is accelerating, rather than inducing, the development of GN in this model.

## INTRODUCTION

Systemic lupus erythematosus (SLE) is a chronic systemic autoimmune disease that can involve multiple organ systems, including the joints, kidneys, skin, brain, cardiovascular system and gastrointestinal system.[1] It is characterized by the production of autoantibodies directed mainly against cellular components, including DNA, chromatin, nucleoproteins, nucleosomes, histones and phospholipids. Renal involvement is one of the most serious complications, and deposition of circulating immune complexes in the glomeruli, or *in situ* formation of immune complexes (IC) in the kidney, result in pathological changes that can lead to potentially fatal renal failure. The incidence of lupus nephritis in patients with SLE, based on an abnormal urinalysis, is approximately 50–70%, but approaches 100% as determined by renal biopsy.[2]

The glomerular lesions associated with lupus nephritis (LN) are heterogeneous and can be classified on the basis of light microscopy, immunofluorescence studies and electron microscopy. Although these classifications are based on histomorphologic characteristics, it is unlikely that they represent distinct pathologic entities, but rather different points in a continuum of disease.[3] The heterogeneity of LN in humans may partially represent both different disease subgroups and different time points in the disease process, but is also contributed to by individual variation in the immunologic responses to autoantigens. Indeed, the renal pathology of an individual can

Received 14 May 2002; revised 27 August 2002; accepted 1 October 2002.

Abbreviations: SLE, systemic lupus erythematosus; BCG, Bacille Calmette–Guérin; EM, electron microscopy; GBM, glomerular basement membrane; GN, glomerulonephritis; IC, immune complex; IF, immunofluorescence; LM, light microscopy; LN, lupus nephritis; MS, methenamine silver; NOD, non-obese diabetic; TP, total protein.

Correspondence: Dr A. G. Baxter, Autoimmunity Research Group, Camparative Genomics Centre, Molecular Sciences Building 21, James Cook University, QLD 4811 Australia. E-mail: Alan.Baxter@JCU.edu.au

transform from one class of LN to another, either spontaneously or following immunosuppressive therapy.[4,5]

The aetiology of SLE is complex and multifactorial, with both environmental and genetic factors known to be involved. Ethnic, family and twin studies in humans, and genetic studies in mice, have demonstrated that SLE, like other autoimmune diseases, is a polygenic trait with contributions from major histocompatibility complex (MHC) genes and multiple non-MHC genes.[6–8] Environmental factors that may trigger or enhance clinical disease include therapeutic drugs such hydralazine[9] ultraviolet radiation[10] and hormonal status (such as pregnancy).[11] The multiplicity of genes and environmental factors contributing to disease expression, coupled with the heterogeneity of the disease phenotype itself, have confounded our understanding of the aetiology and pathogenesis of SLE. Animal models, for which the genetic and environmental factors can be controlled and manipulated, are therefore of particular importance in the dissection of this complex syndrome.

Spontaneous models of inherited LN such as the New Zealand Black × New Zealand White (NZBW) hybrid, BSXB and MRL murine models have contributed greatly to our understanding of some of the pathogenic mechanisms leading to autoimmune disease.[12] Secondary genetic enhancers or accelerators of disease, including the *lpr* and *gld* loci, have revealed the importance of processes such as apoptosis in the loss of tolerance to self antigens in these models.[13,14] Congenic, transgenic and knockout models have also been extensively used to further define and investigate the immunologic pathways and mechanisms important in the pathogenesis of LN (reviewed in 15).

Environmental enhancers of autoimmunity act upon individuals with susceptible genetic backgrounds to increase the penetrance and/or severity of overt disease, and/or accelerate the onset or time course of the disease. Many chemical, metal ion or pharmacological agents can induce glomerulonephritis (GN) in susceptible rodent strains.[16,17] Immunization of mice with self antigens in the presence of adjuvant, transfer or depletion of lymphocyte subpopulations, and induction of chronic graft vs. host disease can also result in systemic autoimmune syndromes.[15] Although these iatrogenic models may have limitations in providing insight into the initial process of loss of self-tolerance, they can nonetheless aid our understanding of the mechanisms of disease progression once the autoimmune process has begun.

Intravenous administration of a single dose of *Mycobacterium bovis* (Bacille Calmette–Guérin; BCG) to young non-obese diabetic (NOD) mice prevents the onset of type 1 diabetes mellitus.[18] However, it precipitates a systemic autoimmune disease similar to SLE and characterized by Coombs' positive haemolytic anaemia (HA), antinuclear antibodies (ANA), increased severity of sialoadenitis and glomerular IC deposition detected by C3c immunofluorescence.[19,20] Although C3c deposition indicates IC glomerulopathy, the exact nature of the renal pathology in BCG-treated NOD mice has not been characterized. The study reported here assessed the morphological and clinical features of renal disease in the NOD mouse model, and examined its suitability as a model for studying the aetiopathogenesis of, and possible treatment options for, lupus nephritis in humans.

## MATERIALS AND METHODS

### *Mice*

Female NOD/Lt mice were obtained from the Animal Resource Center (Canning Vale, WA, Australia) and housed in clean conditions in the animal facility of the Centenary Institute (Sydney, Australia). Sentinel mice were tested by serology at 4-monthly intervals for a panel of viral, bacterial and mycoplasmal pathogens. No sentinel mice tested positive for any of these pathogens.

### *BCG injections*

Mice were injected intravenously via the lateral tail vein at eight weeks of age with 0·6 mg of heat-killed BCG for percutaneous vaccination (CSL, Melbourne, Australia). Dried BCG was washed twice in sterile PBS (Trace Scientific, Clayton, Victoria, Australia), pasteurized at 65° for 40 min, sonicated at 50% of maximum energy for 40 s using a Branson Sonifier 250 (Branson Ultrasonics, Danbury, CT) and resuspended in phosphate-buffered saline (PBS) at a final concentration of 0·6 mg per 200 µl.

### *Light microscopy*

Mice were killed at 250 days (BCG-treated or untreated) or 500 days (untreated) and the kidneys removed. Renal tissue for light microscopy studies was fixed in 10% neutral buffered formalin (Sigma, St Louis, MO). Paraffin-embedded specimens were serially sectioned at 2 µm and stained with haematoxylin and eosin (H&E) and periodic acid–Schiff (PAS). Trichrome and methenamine silver stains (MS) were used to highlight glomerular lesions as required.

### *Direct immunofluorescence*

Kidneys for immunofluorescence studies were snap frozen in Tissue-Tek O.C.T. compound (Miles Inc., Bloomington, IN) and stored at −70°. Five µm cryostat sections were fixed in acetone, and direct immunofluorescence staining performed using tetramethyl rhodamine isothiocyanate (TRITC)-conjugated goat anti-mouse immunoglobulin M (IgM), IgG and IgA antibodies (Southern Biotechnology, Birmingham, AL) and anticomplement C3c conjugated to fluoroscein isothiocyanate (FITC; Nordic Immunology, Tilburg, the Netherlands). After rehydrating the sections in PBS, they were treated with 10% normal horse serum for 20 min, excess serum was blotted from around the sections, and the appropriate antibodies added. The samples were incubated in humidified chambers at room temperature for 30 min, washed three times for 5 min in PBS, mounted and examined using a fluorescence microscope.

### *Electron microscopy*

Renal cortical tissue was cut into 1-mm cubes, fixed in 4% paraformaldehyde, 0·1% glutaraldehyde, 4% sucrose in Hepes-buffered saline, pH 7·4 (150 mM NaCl, 50 mM Hepes, 4 mM $MgCl_2$, 4 mM $CaCl_2$, and 2 mM KCl) and stored at 4°. Tissue was postfixed in 1% $OsO_4$ (aq) for 1 hr, rinsed in milli-Q water and dehydrated in a graded series of acetones (10 min each in 30%, 50%, 15 min in 70%, 10 min in 90% and 95%, then 4 × 15% in absolute dry acetone). Samples were then infiltrated with, and embedded in, Polarbed 812 (ProSciTech, Thuringowa,

Queensland, Australia), and polymerized at 65° for 16 hr. Ultrathin sections (75 nm) were cut on a Reichert Ultracut E (Leica Instruments Ltd, The Patch, Victoria, Australia) using a Diatome diamond knife, collected on copper grids and contrasted with 10% uranyl acetate in 75% methanol, and lead citrate.

*Urinalysis and serum biochemistry*

Mice were monitored monthly for diabetes, HA and ANA production as previously described.[21] Blood glucose readings greater than 11·1 mM on two consecutive readings were considered indicative of diabetes. Diabetic animals were excluded from the study.

Semiquantitative determination of urinary protein and blood was performed on undiluted voided urine samples using Neostix N (Bayer Diagnostics, Mulgrave, Victoria, Australia) or on urine diluted 1 in 30 with sterile distilled water using Clinitek Microalbumin reagent strips read on a Clinitek 50 analyzer (Bayer Diagnostics, Mulgrave, Victoria, Australia). Serum samples were analysed for total protein (TP), albumin, globulin, creatinine and urea using a Roche Cobas Mira Analyzer (Tegimenta, Switzerland).

*Semiquantitative scoring of renal pathology*

A renal score was calculated for each mouse by combining scores for structural and immunofluorescence parameters. As some mice from all strains tested develop mild immunoglobulin deposits with time, structural changes such as mesangial cell proliferation and matrix expansion were weighted more heavily. Mesangial cell proliferation was scored as 0 (absent), 1 (mild), 2 (moderate) or 3 (severe). Mesangial matrix expansion was scored as 0 (absent), 0·5 (mild), 1 (moderate) or 2 (severe). Interstitial infiltrates were classed as 0 (absent), 0·5 (mild) or 1 (significant). Immunofluorescence staining for each of the four isotypes tested was scored as 0 (absent), 0·5 (mild staining of less than 50% of the glomerular tuft) or 1·0 (staining of >50% of the glomerular tuft).

## RESULTS

### Immune complex GN of BCG-treated NOD mice displays a wide spectrum of disease by light microscopy

Histological examination of renal sections from 250-day-old-unmanipulated NOD mice ($n = 10$) revealed grossly normal glomeruli in all mice (Fig. 1a). In contrast, glomerular abnormalities were identified with light microscopy in 12/17 (71%) of BCG-treated NOD mice at 250 days of age, ranging from mild mesangiopathic changes to severe mixed pattern GN. Both global and segmental proliferative lesions, characterized by increases in mesangial matrix and cellularity, were noted, with occasional mesangial nodularity (Fig. 1b). In severely affected glomeruli, obliteration of the capillary lumina, advanced sclerosis and glomerular collapse were apparent.

In addition to the glomerular changes described, all BCG-treated NOD mice displayed paravenular lymphoplasmacytic infiltrates, which were quite florid in some cases (Fig. 1c). Varying degrees of focal interstitial nephritis and tubular mononuclear infiltration were also noted. In contrast, only very mild

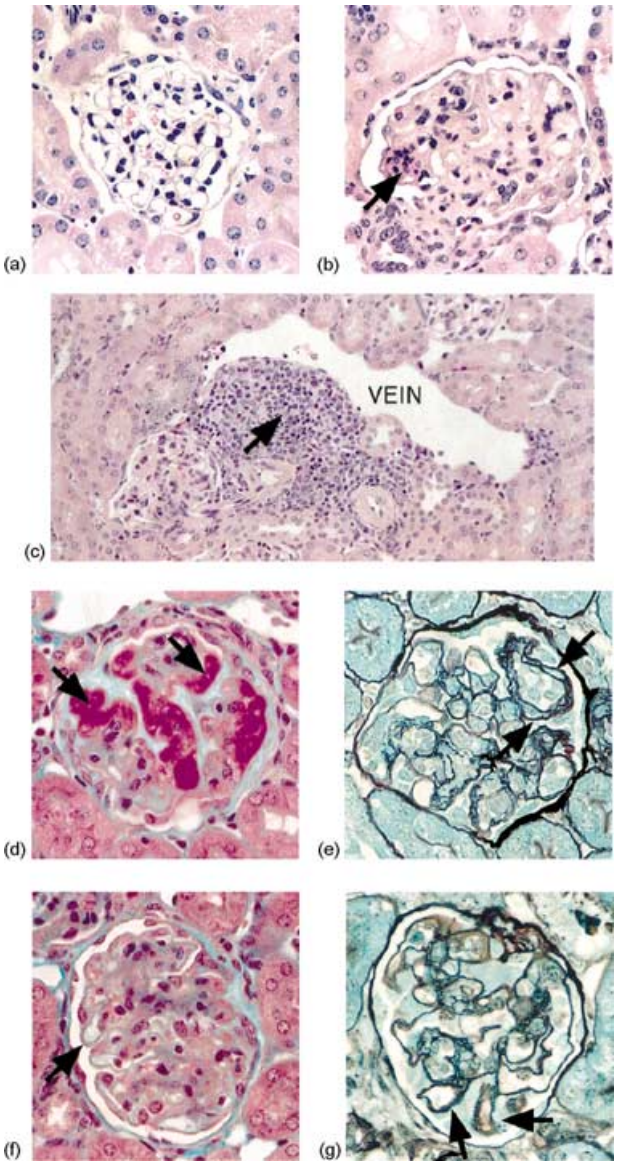


**Figure 1.** Light microscopic changes in renal tissue of BCG-treated NOD mice at 250 days. (a) Glomerulus from an untreated NOD mouse at 250 days, which appears normal on LM (H&E). (b) Mesangiopathic changes in a glomerulus from a BCG-treated NOD mouse, associated with global mesangial proliferation, obliteration of the capillary lumina, and an area of focal mesangial proliferation (arrow) (H&E). (c) Paravenular lymphoplasmacytic infiltrate in a BCG-treated NOD mouse (arrow) (H&E). (d) Large subendothelial deposits (arrows) obliterating the glomerular capillary lumina in a BCG-treated NOD mouse (Trichrome). These extremely fuschinophilic deposits resemble the so-called 'wire-loop' pattern characteristic of mesangiocapillary LN in humans. (e) Reduplication of the GBM resulting in double contouring (arrows) (MS). (f) Subepithelial deposits visible as small fuschinophilic 'beads' along the extraluminal surface of the GBM, consistent with membranous GN (arrow) (Trichrome). Global mesangial proliferation is also present. (g) Proliferation of the GBM between subepithelial deposits results in a 'spike' pattern (arrows) (MS).

**Table 1.** Renal scores for histological and immunofluorescent parameters in BCG-treated NOD mice, control mice, and senescent NOD mice

| Parameter (scoring scale) | C57BL/6 (250 days) | NOD/Lt (250 days) | NOD/Lt (250 days) + BCG | NOD/Lt (500 days) |
|---|---|---|---|---|
| Mesangial cell proliferation (0–3) | 0 ± 0 | 0 ± 0 | 1·12 ± 0·26 | 2·0 ± 0·21 |
| Mesangial matrix expansion (0–2) | 0 ± 0 | 0 ± 0 | 1·03 ± 0·2 | 2·0 ± 0 |
| Interstitial infiltration (0–1) | 0·06 ± 0·06 | 0·35 ± 0·08 | 1·00 ± 0 | 1·00 ± 0 |
| IgM (0–1) | 0·61 ± 0·14 | 0·45 ± 0·16 | 0·76 ± 0·09 | 0·55 ± 0·16 |
| IgG (0–1) | 0·17 ± 0·08 | 0·4 ± 0·15 | 0·85 ± 0·08 | 0·35 ± 0·15 |
| IgA (0–1) | 0·11 ± 0·07 | 0 ± 0 | 0·65 ± 0·09 | 0·1 ± 0·1 |
| C3c (0–1) | 0 ± 0 | 0 ± 0 | 0·44 ± 0·12 | 0·15 ± 0·08 |
| Total (0–10) | 0·94 ± 0·18 | 1·20 ± 0·19 | 5·85 ± 0·62 | 6·25 ± 0·48 |

paravenular infiltrates were identified in some untreated mice of the same age.

Deposits of eosinophilic material were seen in some glomeruli, and appeared strikingly fuschinophilic with trichrome staining, suggesting the presence of immunoglobulin (Fig. 1d). Double contours and epimembranous spikes (the so-called 'spike pattern') were visible with MS staining, findings that suggest mesangiocapillary (Figs 1d,e) and membranous (Figs 1f,g) GN, respectively.

Although there was a range in the severity of the histological changes seen in the BCG-treated group, the changes were more severe than in both the untreated and control groups (Table 1).

### Electron microscopy confirms a mixed site pattern of dense deposits in BCG-treated NOD mice

The light microscopy findings of varying degrees of proliferative and sclerotic glomerular changes were confirmed by electron microscopy. Loss of capillary lumina and glomerular collapse were marked in some sections. Dense deposits were present in subepithelial, intramembranous and subendothelial, positions within thickened glomerular basement membranes (GBM) (Fig. 2). Reduplication of the GBM around some subepithelial dense deposits confirmed the spikes seen with MS staining. Resorption of intramembranous dense deposits resulting in lucent deposits gave the GBM a motheaten appearance in some areas. Foot process effacement was present over segments of GBM that contained subepithelial dense deposits or exhibited spikes or sclerotic changes. Widening of the subendothelial space (lamina rara interna) and evidence of early GBM interpositioning by mesangial cell processes was also seen.

Mesangial areas showed varying degrees of expansion and contained dense deposits of varying size along with hypertrophic cells. In one area organized or crystalline deposits were present (Fig. 2d). No tubuloreticular inclusions were seen.

### Glomerular immune complexes in BCG-treated NOD mice consist of multiple immunoglobulin isotypes

Direct immunofluorescence studies confirmed the glomerular deposits to be immune complexes, with IgG, IgM and IgA identified. Deposits were found in both the mesangium and the peripheral capillary loops, where they showed a granular pattern (Fig. 3a). Most BCG-treated mice had multiple Ig isotypes present, with 76% displaying all three isotypes simultaneously (Table 2). Glomerular C3c staining was positive in 47% of animals (Fig. 3b), and colocalized with the immunoglobulin deposits (Fig. 3c). Occasional focal immune deposits were also found associated with tubular basement membranes on immunofluorescence.

### Spontaneous mixed isotype IC GN occurs in senescent NOD mice

Although unmanipulated NOD mice showed no glomerular changes upon light microscopy at 250 days of age, by 500 days all mice showed at least some glomerular abnormalities on H&E and PAS-stained sections. At 250 days of age, IgM and IgG deposits were demonstrated in the glomeruli of 50% and 40% of untreated mice, respectively, although C3c and IgA were not detected (Tables 1 and 2). In contrast, both C3c and IgA were identified at 500 days. One mouse displayed deposition of C3c together with all three immunoglobulin isotypes at 500 days, confirming that 'full house' mixed isotype immune complexes can occur spontaneously in aged NOD mice.

**Table 2.** Proportion of NOD/Lt mice with positive kidneys on immunofluorescent staining

| Age (days) | Treatment | *n* | % IgG | % IgM | % IgA | % all Ig | % C3c |
|---|---|---|---|---|---|---|---|
| 250 | None | 10 | 40 | 50 | 0 | 0 | 0 |
| 250 | BCG | 17 | 88 | 88 | 82 | 76 | 47 |
| 500 | None | 10 | 40 | 60 | 10 | 10 | 30 |

Ig, immunoglobulin.

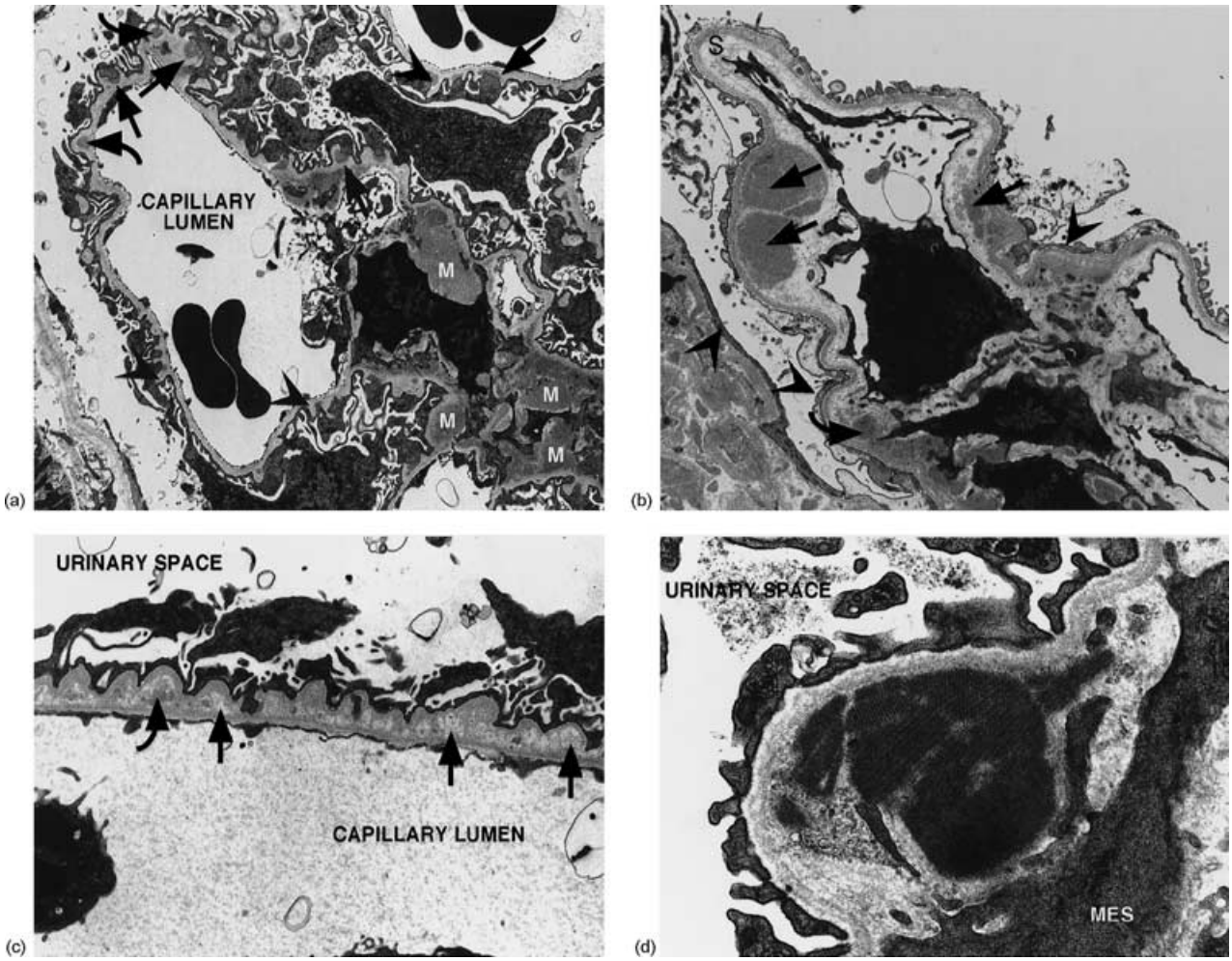


**Figure 2.** Ultrastructural changes in renal tissue of BCG-treated NOD mice at 250 days. (a) Electron micrograph of a glomerulus showing a mixed membranous/mesangial pattern of dense deposits. Subepithelial (straight arrows), intramembranous (curved arrows) and mesangial (M) deposits are present, along with GBM spikes (arrowheads). Mag: 2800×. (b) Electron micrograph of a glomerulus showing subendothelial (straight arrows) and mesangial (curved arrows) dense deposits. There is expansion of the subendothelial space or lamina rara interna (S) and effacement of foot processes, particularly over a collapsed segment (arrowheads). Mag: 5400×. (c) Electron micrograph of a segment of GBM showing intramembranous lucent deposits (straight arrows) and partially resorbed dense deposits exhibiting a lucent halo (curved arrows). Foot processes show effacement and podocytes forming microvilli. Mag: 5550×. (d) Electron micrograph of an organized, or crystalline, mesangial dense deposit. MES: mesangial cell. Mag: 20 500×.

### Urinalysis and serum biochemistry results do not accurately reflect the severity of glomerular pathology in BCG-treated NOD mice

All mice in the study, including untreated controls, had proteinuria detectable using Neostix N strips, consistent with the physiological proteinuria previously reported in mice.[22] In an attempt to overcome interference by physiological proteinuria, Clinitek Microalbumin test strips, which are described as specific for albumin in humans (Clinitek Microalbumin data sheet, Bayer Diagnostics, Mulgrave, Victoria, Australia), were used. However, urine from healthy NOD/Lt, BALB/c and C57BL/6 mice aged between 4 and 24 weeks revealed that mouse urine reacts strongly and consistently with the 'albumin-specific' reagent strip, indicating significant albuminuria is present, and/or that species-specific proteins may be cross reacting with the test reagent. Dilution of urine at 1 in 30 in distilled water was necessary to reduce this constitutive reaction to baseline levels (10 mg/l).

As reference ranges for biochemical parameters for NOD mice needed to be established for the laboratory we are using, serum samples from 35 non-diabetic adult female mice were tested for total protein (TP), albumin, globulin, creatinine and urea. The normal ranges, calculated as mean $\pm 1{\cdot}96$ SD, are shown in Table 3. All BCG-treated NOD mice showed increased TP (range 63·8–75·9 g/l), which was due to an increase in the globulin fraction (range 32·8–42·2 g/l). However, the remaining clinical parameters were within normal limits in most BCG-treated mice. Slightly low serum albumin (26·8 g/l) was found in only one mouse with moderate glomerular

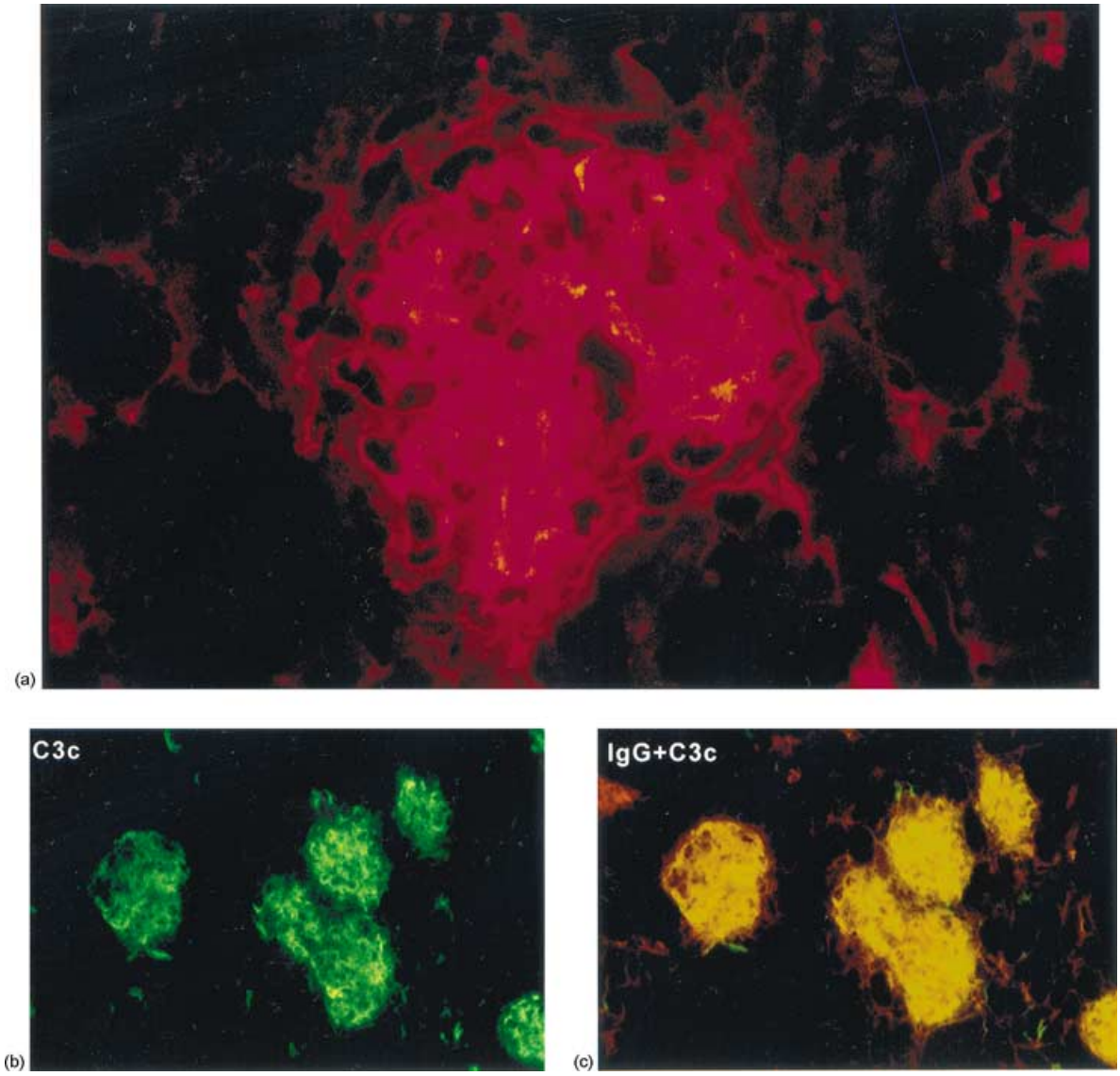


**Figure 3.** Direct immunofluorescence of renal tissue from BCG-treated NOD mice at 250 days. (a) IgA deposits in a glomerulus showing mixed mesangial and glomerular capillary wall staining. (b) C3c is deposited both in the mesangium and along the capillary wall. (c) Colocalization of IgG (TRITC) and C3c (FITC) demonstrated by areas of yellow fluorescence.

pathology, however, this was not accompanied by a detectable increase in urinary albumin excretion. One BCG-treated mouse with very severe GN, resembling fulminant diffuse mixed site LN in humans, had increased serum urea (19·1 mmol/l), accompanied by hematuria and marked proteinuria demonstrated with both urinalysis methods. Urinalysis was unremarkable in all other animals, including those with significant morphological GN.

**Table 3.** Reference ranges for serum biochemical parameters in female NOD mice

| Parameter | Mean | SD | Reference range |
|---|---|---|---|
| Total protein (g/l) | 56·59 | 2·36 | 52·0–61·2 |
| Albumin (g/l) | 31·41 | 1·66 | 28·2–34·7 |
| Globulin(g/l) | 25·18 | 2·03 | 21·2–29·2 |
| Creatinine (mmol/l) | 27·86 | 5·13 | 18–38 |
| Urea(mmol/l) | 7·97 | 1·28 | 5·46–10·47 |

## DISCUSSION

This is the first comprehensive study of the glomerular pathology precipitated in NOD mice by administration of mycobacteria. As human LN can mimic nearly any histomorphologic type of primary glomerulopathy, the combination of all morphologic modalities routinely used in the interpretation of human renal biopsies (i.e. light microscopy, electron microscopy and immunofluorescence) was required to assess the validity of this murine model of LN.

Light microscopic findings such as mesangial proliferation, basement membrane changes and deposition of fuschinophilic material were suggestive of IC GN in BCG-treated NOD mice. Immunofluorescence demonstrated the presence of mixed isotype ICs (including the 'full house' of immunoglobulin isotypes) in individual animals. Ultrastructural examination confirmed these deposits were located in mesangial, paramesangial, subendothelial, subepithelial and intramembranous sites within the glomeruli. These findings strongly resemble the pathology seen in human LN, with changes characteristic of the continuum of LN, including mesangiopathic, mesangiocapillary and membranous patterns. Although tubuloreticular inclusions were not seen in our model, the presence of organized or crystalline dense deposits similar to those seen in the present study is highly specific for LN in humans.[23] The pathological changes observed were consistent with, but were not of themselves diagnostic of, lupus.

Spontaneous IC GN, characterized by positive immunofluorescence for IgG and C3c, has been widely studied in mouse strains such as NZBW hybrid, BSXB and MRL. Progressive mesangial proliferation, lobulation of the glomerular tuft, marked and irregular thickening of the GBM, obliterative sclerosis and interstitial mononuclear infiltration develop in NZBW and MRL/lpr mice.[12,24] In NZBW mice, electron dense IC deposits are found within and on both sides of the GBM.[25] Similar to the BCG-induced model, varying combinations and grades of lesions are seen between and within individual animals.[24] Although fibrinoid and florid crescentic lesions are common in the NZBW and MRL/lpr, these were not identified in this model. The IC GN that develops in male BXSB mice is also characterized by proliferative glomerular changes, but this is accompanied by exudation of neutrophils into the glomeruli,[26] which is an unusual finding in LN.

Hematuria and albuminuria are hallmarks of glomerular disease. Assessment of abnormal albuminuria in mice using routine test strips was complicated by the presence of constitutive proteinuria and albuminuria.[22] Standard dry reagent urine protein test strips, such as Neostix N and Albustix, use tetrabromophenol blue as the protein reactive agent, which does not distinguish albumin from other proteins such as globulin, haemoglobin, Bence-Jones protein or mucoprotein (data sheet, Bayer Diagnostics, Mulgrave, Victoria, Australia). Clinitek Microalbumin reagent strips use a sulfonephthalein dye which does not react with these other proteins in human urine. However, our results, derived using multiple mouse strains at varying ages, revealed that normal mouse urine reacts strongly and consistently with the 'albumin-specific' reagent strip indicating significant physiological albuminuria is present. Hoffsten *et al.* (1975) measured the amount of albuminuria in normal SWR/J mice by radial immunodiffusion, and calculated an upper limit of normal as 0·4 mg per 18 hr (mean + 2SD).[22] It is also possible that other species-specific urinary proteins may be cross-reacting with the test reagent. Dilution of urine at 1 in 30 in distilled water reduced this constitutive reactivity to baseline levels (10 mg/l) in control mice, but reduced the sensitivity of the assay.

In the present study, clinical parameters of GN and renal insufficiency, such as hematuria, increased albuminuria and azotemia were rarely present, even in animals with quite pronounced GN on morphological examination. In a study of IC GN induced by lymphocytic choriomeningitis (LCM) virus infection in SWR/J mice, albuminuria measured by radial immunodiffusion was not abnormal in 75% of infected mice, even in the presence of marked glomerular pathology.[22] Similarly, in human patients with SLE, it is widely reported that urinalysis findings and serology do not always reflect the presence of LN, and severe changes can be found on renal biopsy in the absence of clinical evidence of renal disease.[27,28] This highlights the importance of renal biopsy in diagnosis of LN in SLE patients who lack definitive serological or urinary signs of renal involvement.

Because of the polygenic, multifactorial etiology and the heterogeneous phenotype of LN, no single animal model of LN can address all the issues involved in understanding the aetiopathogenesis of this disease. While models with high spontaneous penetrance of a relatively homogeneous phenotype, such as the NZBW, assist in genome mapping and identification of susceptibility loci, models with well characterized environmental contributions, such as NOD mice, allow study of interactions between genetic and environmental factors influencing the autoimmune phenotype.[29]

Environmental enhancers of disease may act through antigen-specific mechanisms, such as molecular mimicry or cross-reactivity, or antigen non-specific mechanisms, such as direct toxicity, adjuvant-like immunostimulation or specific enhancement of certain cytokine profiles. It is unlikely that molecular mimicry is a significant mechanism of action by which mycobacteria precipitate SLE-like disease in NOD mice because of the large variety of target autoantigens identified, including DNA, Sm and surface red blood cell antigens.[20] ANA do not arise from cross-reactivity with *M. bovis* antigens, as there is no correlation between ANA and anti-*M. bovis* IgG titres in treated mice.[30] Similarly, skewing of the autoimmune response towards a T helper 2 (Th2)-type profile is also not a predominant mechanism since treated mice show several features typical of both a Th1 response, including enhanced delayed-type hypersensitivity (DTH) and an IgG2a anti-Sm autoantibody profile.[19] In contrast, it appears that an adjuvant-like effect results in recruitment of large numbers of antigen presenting cells and enhanced antigen presentation to T cells, thus accelerating the onset of spontaneous systemic autoimmunity in this model.[19]

The effect of genetic and environmental enhancers of autoimmunity is strongly influenced by the genetic background. For example, the *lpr* and *gld* mutations in Fas and FasL, respectively, cause severe GN in MRL mice, but not in C3H mice.[31] As MRL mice naturally develop weak and delayed GN, these genes are acting as enhancers or accelerators of autoimmunity, rather than inducing autoimmunity *per se*. Similarly, although female BXSB mice develop late onset IC GN, the Y-linked *Yaa* gene greatly enhances and accelerates disease in male BXSB mice.[26] The influence of environmental agents such as lead and mercury in precipitating LN is also dependent on an underlying genetically susceptible background.[29,32,33]

The progressive development of spontaneous mixed isotype IC GN in the glomeruli of senescent NOD mice suggests that BCG is accelerating, rather than inducing, the development of GN. Previous reports that other lupus-associated pathologies, such as HA and ANA production, also occur spontaneously in

aged NOD mice[30,34–36] and are precipitated by BCG treatment[19,20] support this theory. Increases in ANA titres and the premature development of Coombs' positive HA were also noted in the BCG-treated NOD mice compared with age-matched controls in this study (data not shown). Therefore this model of LN may be of great use in dissecting the interaction between genetic susceptibility to autoimmunity (NOD genetic background) and an environmental accelerator or enhancer (mycobacteria).

The NOD mouse model has the advantage that it is genetically well characterized, particularly with respect to genes associated with autoimmunity.[37,38] Our recent linkage study has identified susceptibility loci for HA and ANA production following BCG administration in this model[21] and some of these loci colocalize with known susceptibility loci for other murine models of SLE. Although significant linkage was not found in this study for glomerular IC deposition, suggestive linkage was reported on chromosomes 1 and 4.

The many congenic and transgenic NOD strains available will allow further dissection of the genetic contributions to LN in this model. Additionally, the modification of the environmental enhancer of LN in terms of strain of mycobacteria, dosage and route of administration may enable better understanding many of the complex gene–environment interactions that influence the penetrance, time course and severity of LN. As the BCG-induced NOD mouse model of LN displays a similar spectrum of pathology to that seen in human LN, it may also afford insights into the response to new therapeutic options, while bypassing the need for serial biopsies in clinical studies of human patients.

## ACKNOWLEDGMENTS

We thank the staff of the animal facility at the Centenary Institute for animal care, and Karen Barnes and Jane Radford for technical assistance. This work was supported by the Australian National Health and Medical Research Council. AGB is supported by an interim fellowship from the Australian National Health and Medical Research Council. CGH is supported by an Australian Postgraduate Award from the University of Sydney. These studies were performed under approval #K75/2-2000/3/3098 of the University of Sydney Animal Ethics Committee.

## REFERENCES

1 Tan EM, Cohen AS, Fries JF *et al.* The 1982 revised criteria for the classification of systemic lupus erythematosus. Arthritis Rheum 1982; **25:**1271–7.
2 Churg J, Bernstein J, Glassock RJ. Renal Disease: Classification and Atlas of Glomerular Diseases. New York: Igaku-Shoin Medical Publishers, Inc 1995.
3 Kashgarian M. Lupus nephritis. Pathology, pathogenesis, clinical correlations and prognosis. In: Wallace, DJ, Hahn, BH, eds. Dubois' Lupus Erythematosus. Baltimore: Williams & Wilkins 1997:1037–51.
4 Baldwin DS, Gluck MC, Lowenstein J, Gallo GR. Lupus nephritis. Clinical course as related to morphologic forms and their transitions. Am J Med 1977; **62:**12–30.
5 Appel GB, Valeri A. The course and treatment of lupus nephritis. Annu Rev Med 1994; **45:**525–37.
6 Theofilopoulos AN, Kofler R, Singer PA, Dixon FJ. Molecular genetics of murine lupus models. Adv Immunol 1989; **46:**61–109.
7 Vyse TJ, Kotzin BL. Genetic susceptibility to systemic lupus erythematosus. Annu Rev Immunol 1998; **16:**261–92.
8 Tan FK, Arnett FC. The genetics of lupus. Curr Opin Rheumatol 1998; **10:**399–408.
9 Cameron HA, Ramsay LE. The lupus syndrome induced by hydralazine: a common complication with low dose treatment. Br Med J (Clin Res Ed) 1984; **289:**410–2.
10 Ansel JC, Mountz J, Steinberg AD, DeFabo E, Green I. Effects of UV radiation on autoimmune strains of mice: increased mortality and accelerated autoimmunity in BXSB male mice. J Invest Dermatol 1985; **85:**181–6.
11 Petri M, Howard D, Repke J. Frequency of lupus flare in pregnancy. The Hopkins Lupus Pregnancy Center experience. Arthritis Rheum 1991; **34:**1538–45.
12 Theofilopoulos AN, Dixon FJ. Murine models of systemic lupus erythematosus. Adv Immunol 1985; **37:**269–390.
13 Watanabe-Fukunaga R, Brannan CI, Copeland NG, Jenkins NA, Nagata S. Lymphoproliferation disorder in mice explained by defects in Fas antigen that mediates apoptosis. Nature 1992; **356:**314–7.
14 Takahashi T, Tanaka M, Brannan CI, Jenkins NA, Copeland NG, Suda T, Nagata S. Generalized lymphoproliferative disease in mice, caused by a point mutation in the Fas ligand. Cell 1994; **76:**969–76.
15 Foster MH. Relevance of systemic lupus erythematosus nephritis animal models to human disease. Semin Nephrol 1999; **19:**12–24.
16 Bigazzi PE. Autoimmunity and heavy metals. Lupus 1994; **3:**449–53.
17 Satoh M, Kumar A, Kanwar YS, Reeves WH. Anti-nuclear antibody production and immune-complex glomerulonephritis in BALB/c mice treated with pristane. Proc Natl Acad Sci USA 1995; **92:**10934–8.
18 Harada M, Kishimoto Y, Makino S. Prevention of overt diabetes and insulitis in NOD mice by a single BCG vaccination. Diabetes Res Clin Pract 1990; **8:**85–9.
19 Baxter AG, Healey D, Cooke A. Mycobacteria precipitate autoimmune rheumatic disease in NOD mice via an adjuvant-like activity. Scand J Immunol 1994; **39:**602–6.
20 Baxter AG, Horsfall AC, Healey D, Ozegbe P, Day S, Williams DG, Cooke A. Mycobacteria precipitate an SLE-like syndrome in diabetes-prone NOD mice. Immunology 1994; **83:**227–31.
21 Jordan MA, Silveira PA, Shepherd DP *et al.* Linkage analysis of systemic lupus erythematosus induced in diabetes-prone nonobese diabetic mice by *Mycobacterium bovis*. J Immunol 2000; **165:**1673–84.
22 Hoffsten PE, Hill CL, Klahr S. Studies of albuminuria and proteinuria in normal mice and mice with immune complex glomerulonephritis. J Laboratory Clin Med 1975; **86:**920–30.
23 Hvala A, Kobenter T, Ferluga D. Fingerprint and other organised deposits in lupus nephritis. Wien Klin Wochenschr 2000; **112:**711–5.
24 Howie JB, Helyer BJ. The immunology and pathology of NZB mice. Adv Immunol 1968; **9:**215–66.
25 Channing AA, Kasuga T, Horowitz RE, Dubois EL, Demopoulos HB. An ultrastructural study of spontaneous lupus nephritis in the NZB-BL-NZW mouse. Am J Pathol 1965; **47:**677–94.
26 Murphy ED, Roths JB. A Y chromosome associated factor in strain BXSB producing accelerated autoimmunity and lymphoproliferation. Arthritis Rheum 1979; **22:**1188–94.
27 Hollcraft RM, Dubois EL, Lundberg GD, Chandor SB, Gilbert SB, Quismorio FP, Barbour BH, Friou GJ. Renal damage in systemic lupus erythematosus with normal renal function. J Rheumatol 1976; **3:**251–61.
28 Grande JP, Balow JE. Renal biopsy in lupus nephritis. Lupus 1998; **7:**611–7.
29 Rudofsky UH, Lawrence DA. New Zealand mixed mice: a genetic systemic lupus erythematosus model for assessing environmental effects. Environ Health Perspect 1999; **107** (Suppl. 5):713–21.

30 Horsfall AC, Howson R, Silveira P, Williams DG, Baxter AG. Characterization and specificity of B-cell responses in lupus induced by *Mycobacterium bovis* in NOD/Lt mice. Immunology 1998; **95:**8–17.
31 Kelley VE, Roths JB. Interaction of mutant *lpr* gene with background strain influences renal disease. Clin Immunol Immunopathol 1985; **37:**220–9.
32 Abedi-Valugerdi M, Hansson M, Moller G. Genetic control of resistance to mercury-induced immune/autoimmune activation. Scand J Immunol 2001; **54:**190–7.
33 Abedi-Valugerdi M, Moller G. Contribution of *H-2* and non-*H-2* genes in the control of mercury-induced autoimmunity. Int Immunol 2000; **12:**1425–30.
34 Baxter AG, Mandel TE. Hemolytic anemia in non-obese diabetic mice. Eur J Immunol 1991; **21:**2051–5.
35 Arai T, Noguchi K, Machida N, Sasaki M, Oki Y, Komeda K. Detection of nuclear protein antigens to antinuclear antibodies in serum of NOD mouse. Jikken Dobutsu 1989; **38:**159–62.
36 Humphreys-Beher MG, Brinkley L, Purushotham KR *et al.* Characterization of antinuclear autoantibodies present in the serum from nonobese diabetic (NOD) mice. Clin Immunol Immunopathol 1993; **68:**350–6.
37 Wicker LS, Todd JA, Peterson LB. Genetic control of autoimmune diabetes in the NOD mouse. Annu Rev Immunol 1995; **13:**179–200.
38 Baxter AG, Cooke A. The genetics of the NOD mouse. Diabetes-Metabolism Rev 1995; **11:**315–35.